

Noise Removal from Multiple MRI Images

S. Garnier
G. Bilbro
W. Snyder
J. Gault

Center for Communications and Signal Processing
Department of Electrical and Computer Engineering
North Carolina State University

TR-94/9
April 1994

(Accepted by JDI; modifications are underway.)

Noise Removal from Multiple MRI Images

Stephen J. Garnier, Griff L. Bilbro, Wesley E. Snyder, James W. Gault

We introduce a novel technique for Magnetic Resonance Image (MRI) restoration, using a physical model (spin equation).

We determine a set of three basis images (proton density and nuclear relaxation times) from the MRI data using a nonlinear optimization method and use those images to obtain excellent restorations of the original image.

Magnetic Resonance Images depend nonlinearly on proton density, PD, two nuclear relaxation times, T_1 and T_2 , and two control parameters, TE and TR. We model images as Markov random fields and introduce a maximum *a posteriori* (MAP) restoration method, based on nonlinear optimization, which reduces noise while preserving resolution.

KEY WORDS: Image Analysis, Magnetic Resonance, Noise removal, Physical Model, Basis Images, Restoration, Markov Random Fields, Optimization.

1.0 Introduction

The “Spin Equation” [1] relates the image signal strength measured at a particular pixel, i , in image c , to three intrinsic properties of a pixel, PD_i , $T1_i$, and $T2_i$, and to two measurement parameters, TE_c , and TR_c :

$$S_{c,i} = PD_i \exp\left(\frac{-TE_c}{T2_i}\right) \left(1 - \exp\left(\frac{-TR_c}{T1_i}\right)\right). \quad (\text{EQ 1})$$

Given a set of such measurements taken at a particular pixel, but with different TE and TR values, one could in principle invert the Spin Equation and solve for PD, $T1$ and $T2$ [2]. These PD, $T1$ and $T2$ images can be used to generate images equivalent to data images obtainable with

different TE and TR parameters, thereby minimizing the MR system time [2][3][4]. Since any TE and TR can be simulated from PD, $T1$, and $T2$, we refer to these three images as “basis” images. The inversion problem, however, is ill-conditioned unless TE and TR are chosen carefully. For arbitrary (but different) choices of TE and TR, a numerical method must be used for the solution. We develop this method by assuming that there exist three unknown images, PD, $T1$ and $T2$. At pixel i , a measure of the difference between a single measurement, $G_{c,i}$, and the physical model from (EQ 1), may be written as

$$H_{c,i} = \frac{1}{2\sigma_c^2} (S_{c,i} - G_{c,i})^2 \quad (\text{EQ 2})$$

where σ_c represents the standard deviation of (assumed) stationary, signal-independent, isotropic uncorrelated additive Gaussian noise [5] on the c -th measurement.

Summing over the measurements and the pixels results in a function

$$H_N = \sum_c \sum_i H_{c,i} \quad (\text{EQ 3})$$

which represents the total difference between the measured data and the images resulting from the estimated PD, $T1$ and $T2$ values. Thus, if we can then find the values of PD, $T1$ and $T2$ which minimize H_N , the “noise energy” term, we will have a good estimate of these values. Such minimization may be accomplished by gradient descent or other numerical techniques.

Minimizing (EQ 3) over the PD, $T1$, $T2$ domain results in a “maximum likelihood” (ML) restoration. If one has prior knowledge of some locally homogeneous characteristic of the surfaces of the PD, $T1$ and $T2$ images, this knowledge can be applied in a “prior energy” term, and a maximum *a posteriori* (MAP) restoration with greater noise-reduction can be achieved. We use a measure of the difference between neighboring pixels to remove noise from the PD,

T1 and T2 images, since we assume that neighboring pixels belonging to the same tissue should appear similar, and should possess similar noise statistics. Our choice for this difference measure is based on our previous experience [6][7] with several approaches towards the nonlinear restoration of images.

For a single pixel of interest, say pixel i , and its surrounding neighborhood, \mathfrak{N}_i , the prior energy for the PD signal may be represented by $E_{PD,i}$, where

$$E_{PD,i} = \frac{\sum_{\eta \in \mathfrak{N}_i} (PD_i - PD_{i+\eta})^2}{2\sigma_{PD}^2 + \frac{1}{\tau} \sum_{\eta \in \mathfrak{N}_i} (PD_i - PD_{i+\eta})^2}. \quad (\text{EQ 4})$$

The value for σ_{PD} , a well chosen estimate of noise in the PD image, indicates the emphasis of smoothing on the PD image. The parameter τ is a smoothly changing annealing parameter. At infinite τ , the prior term performs simple linear smoothing; a low-pass filter. As τ is decreased, the influence of the prior term gives way to the noise term, and the restoration takes on the appearance of the ML solution as $\tau \rightarrow 0$.

We refer to the prior term of (EQ 4) as a ‘‘Signal-OR, Spatial-AND’’ formulation. There are several other forms which we have used for this prior term, but this will be the only form discussed here. In any case, the prior energy formulations for T1 and T2 are isomorphic to that of PD.

Summing the prior energy contributions results in a function

$$H_p = \sum_i (E_{PD,i} + E_{T1,i} + E_{T2,i}) \quad (\text{EQ 5})$$

which represents a degree of smoothness within a local region of the PD, T1 and T2 images. Thus, if we can find values for PD, T1 and T2 which minimize

$$H = H_N + H_p \quad (\text{EQ 6})$$

at each value of τ , starting at a high value for τ , and halting the process when τ is small enough, we will obtain a restoration which retains fidelity to the data, preserves step edges, and suppresses noise.

2.0 Methods

We acquired several sets of three images each from a GE Signa 5.2 scanner with a 1.5 Tesla magnet using spin-echo mode, acquiring one T1-weighted study and one PD/T2-weighted multi-echo study for a total of three images per set. TE and TR values set for the presumably healthy brain in the left half of Figures 1 through 3 were (TE,TR) = (32,3000), (90,3000) and (17,500). This particular image set was obtained from a study using 3mm gaps between adjacent 3mm slices with a field of view of 22cm.

The brain images which show pathology in the left half of Figures 4 through 6 were obtained after administration of Gadolinium. The TE and TR values were set at (32,3000), (90,3000) and (17,417). This study used 1mm gaps between 5mm slices. The field of view was set at 22cm.

The noisy images of a presumably healthy brain in the left half of Figures 7 through 9 used (TE,TR) settings of (30,900), (90,900) and (90,1800). This study used 0mm gaps between 3mm slices. Again, the field of view was fixed at 22cm.

All of these data images were processed using both the ML and MAP algorithms. The H of (EQ 6) was minimized with respect to PD, T1, and T2 using gradient descent. See[7] for details. Since only three data images were used during each restoration, the ML restorations showed no improvement over the data. Values for the σ_c in the noise term were estimated from a region of tissue in each acquired image which appeared to have an underlying piecewise-constant value. Values for σ_{PD} , σ_{T1} and σ_{T2} were similarly determined from a region of tissue in each ML-restored basis image which also appeared to have an underlying piecewise-constant value.

3.0 Results

The images in the right half of Figures 1 through 9 are the synthetic restorations produced by the MAP algorithm. The σ_c , σ_{PD} , σ_{T1} and σ_{T2} were all determined from white-matter regions. We also used σ_{PD} , σ_{T1} and σ_{T2} determined as a fraction of the mean value from their corresponding white-matter signals in an effort to model an equivalent degree-of-smoothness across all basis images, but found the restorations to be visually equivalent to those presented here. Intensity differences between the data and the

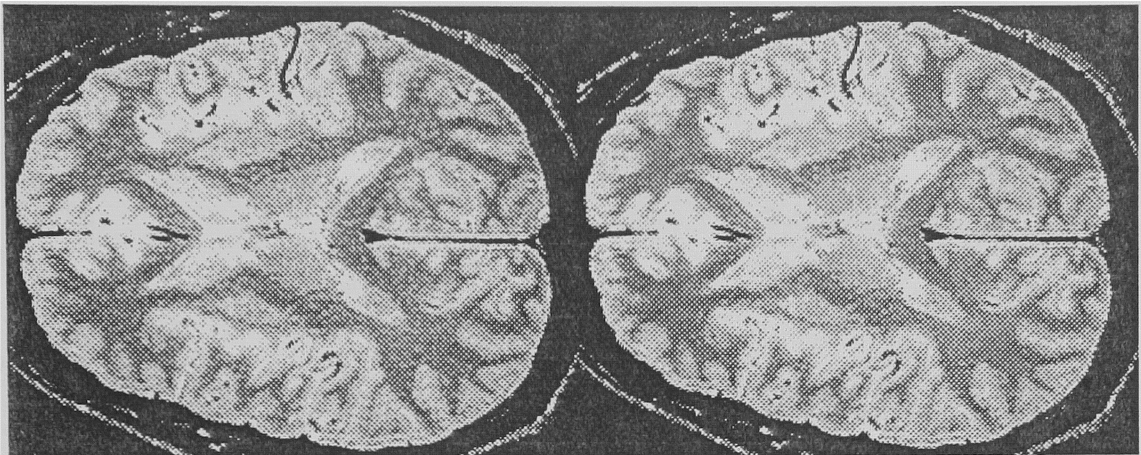


FIGURE 1. $TE = 32$, $TR = 3000$. Left: Data, Right: MAP Restoration. 3mm slice with 3mm spacing.

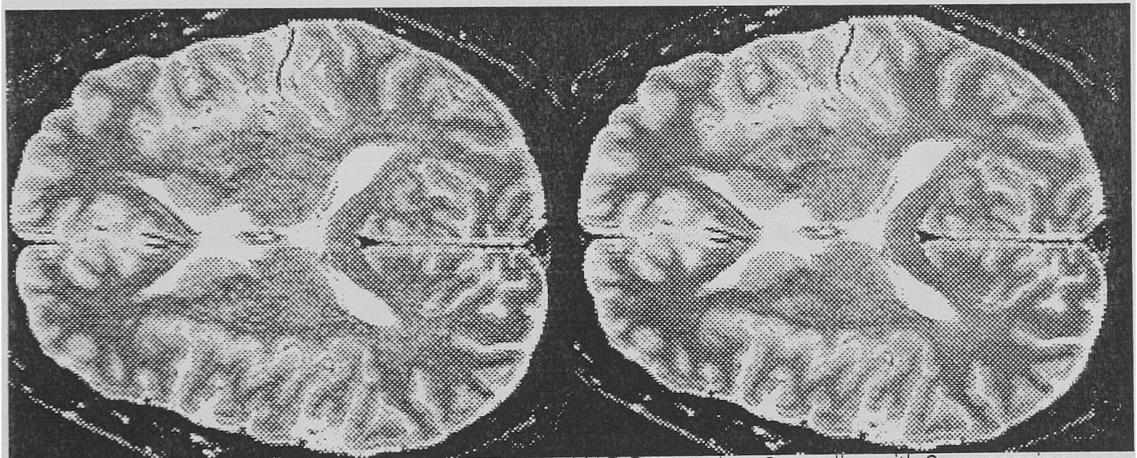


FIGURE 2. $TE = 90$, $TR = 3000$. Left: Data, Right: MAP Restoration. 3mm slice with 3mm spacing.

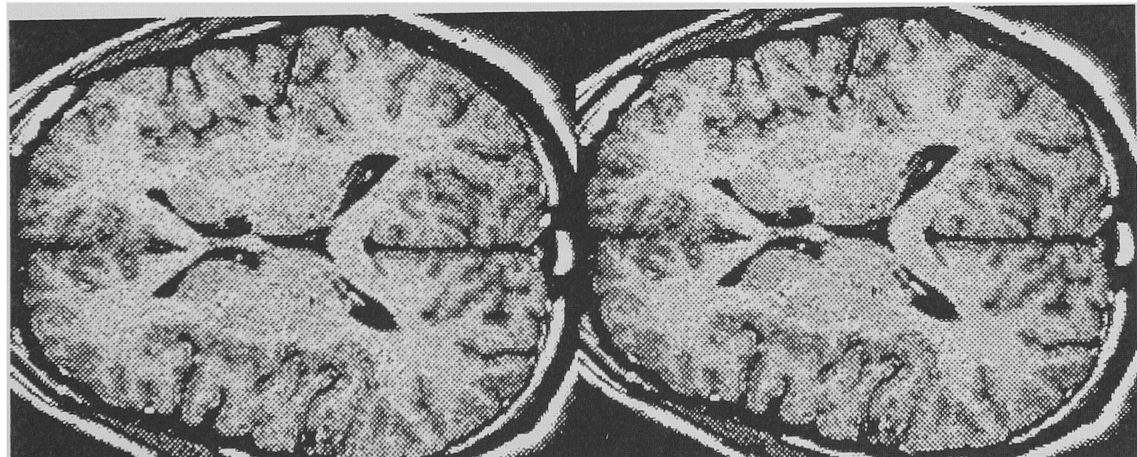


FIGURE 3. $TE = 17$, $TR = 500$. Left: Data, Right: MAP Restoration. 3mm slice with 3mm spacing.



FIGURE 2. $TE = 90$, $TR = 3000$. Left: Data, Right: MAP Restoration. 3mm slice with 3mm spacing.



Results

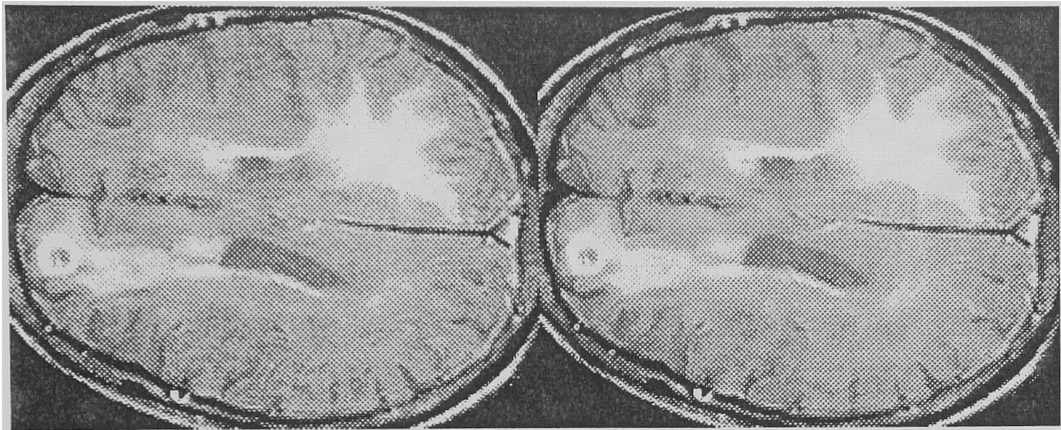


FIGURE 4. TE = 32, TR = 3000. Left: Data, Right: MAP Restoration. 5mm slice with 1mm spacing. Gadolinium administered prior to study.

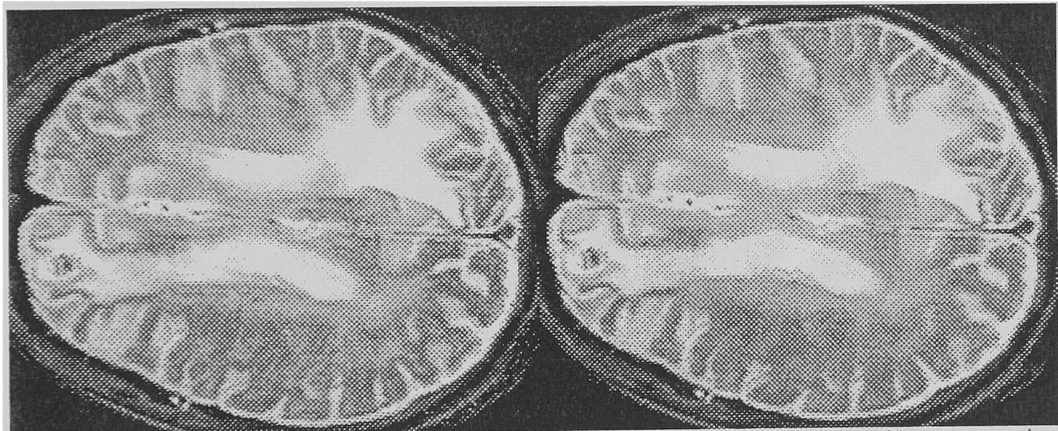


FIGURE 5. TE = 90, TR = 3000. Left: Data, Right: MAP Restoration. 5mm slice with 1mm spacing. Gadolinium administered prior to study.

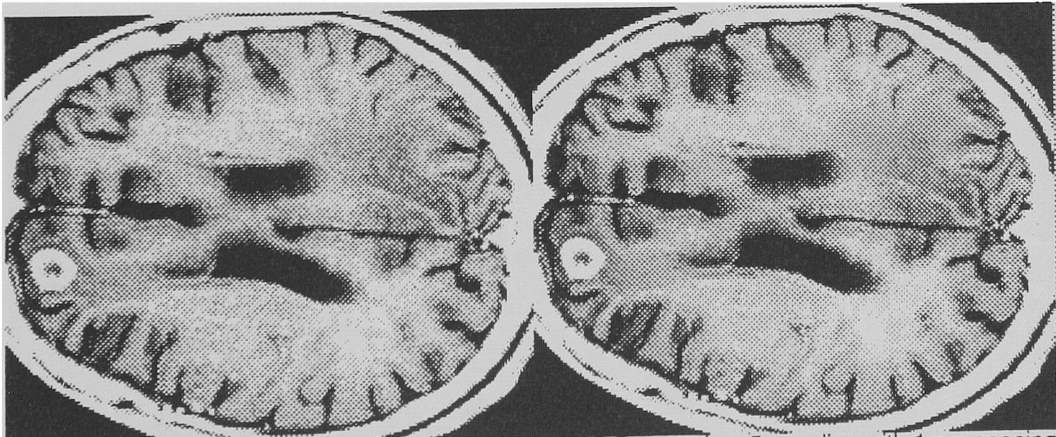


FIGURE 6. TE = 17, TR = 417. Left: Data, Right: MAP Restoration. 5mm slice with 1mm spacing. Gadolinium administered prior to study.



FIGURE 5. TE = 90, TR = 3000. Left: Data, Right: MAP Restoration. 5mm slice with 1mm spacing. Gadolinium administered prior to study.



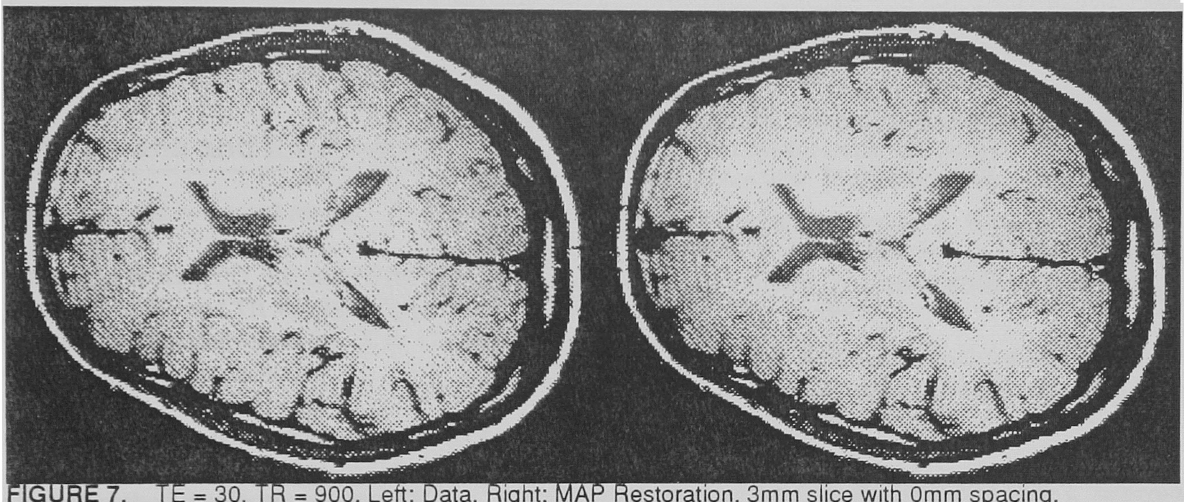


FIGURE 7. TE = 30, TR = 900. Left: Data, Right: MAP Restoration. 3mm slice with 0mm spacing.

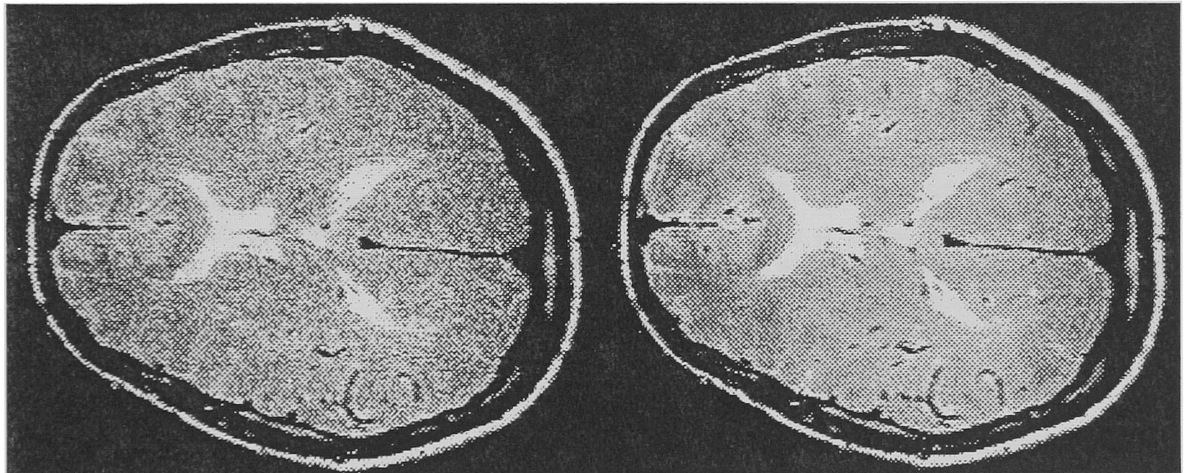


FIGURE 8. TE = 90, TR = 900. Left: Data, Right: MAP Restoration. 3mm slice with 0mm spacing.

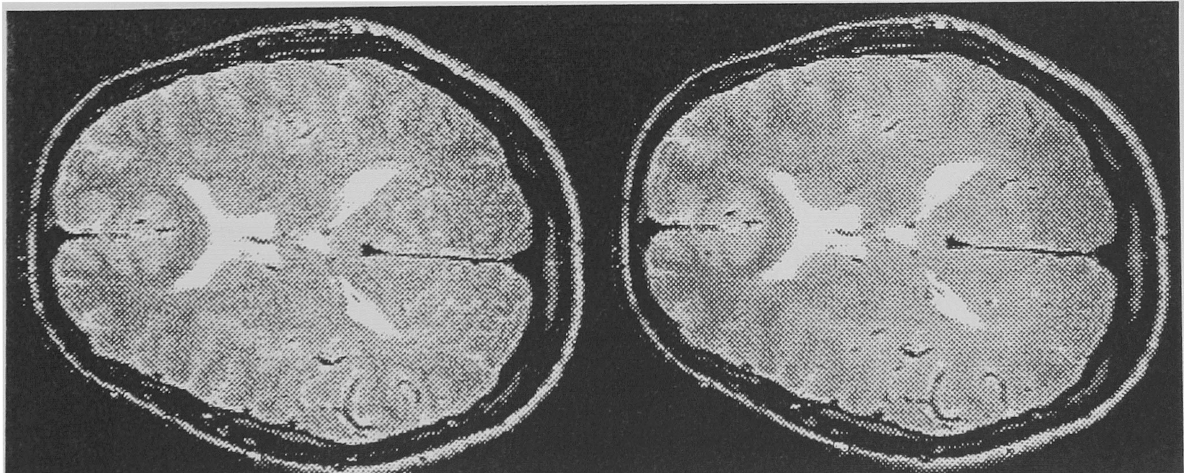


FIGURE 9. TE = 90, TR = 1800. Left: Data, Right: MAP Restoration. 3mm slice with 0mm spacing.



FIGURE 8. TE = 90, TR = 900. Left: Data, Right: MAP Restoration. 3mm slice with 0mm spacing.

restorations are an artifact of photographic processing and printing.

4.0 Conclusions and future work

We have demonstrated two novel results:

1) A method of computing PD, T₁, and T₂ from any set of images with distinct TE and TR values. All previous reported work chose special values for TE or TR which simplified the coupled spin equations.

2) A method for removing noise (while still preserving the sharpness of edges) from these images which seems to be superior to any method previously reported [7].

When used in the spin-echo application, the method suffers from the requirement that the patient must remain motionless between the multiple studies which use dissimilar TR values.

Although demonstrated using readily available spin-echo images, the method is readily adaptable to other MRI imaging modes by simply changing the form of the physical relation equation.

It may be argued that in conventional spin-echo, noise-like artifacts arise primarily from metabolic motion and are not (for the most part) from true random noise. However, in EPI images, acquisition times are so short that motion artifacts are dramatically reduced and to some extent replaced by random noise (with which this algorithm performs best). In imaging using an MTC preparatory pulse, the formation equation has a form similar to (EQ 1), and this method should be applicable to removing noise from such images. Investigations are under way.

5.0 Acknowledgements

This work was supported by the U. S. Army Research Office under Contract DAAL03-89-D-0003-0004 and by the Center for Communications and Signal Processing, North Carolina State University. We would like to express our gratitude to W. H. Hinson and C. A. Hamilton at the Bowman-Gray School of Medicine, Wake Forest University, for providing data images.

6.0 References

1. J. Liu, A. O. K. Nieminen, and J. L. Koenig. Calculation of T₁, T₂, and proton spin density images in nuclear magnetic resonance imaging. *Journal of Magnetic Resonance*, 85:95-110, 1989.
2. D. A. Ortendahl, N. Hylton, L. Kaufman, J. C. Watts, L. E. Crooks, C. M. Mills, and D. D. Stark. Analytic tools for magnetic resonance imaging. *Radiology*, 153(2):479-488, 1984.
3. J. N. Lee, S. J. Riederer, S. A. Bobman, F. Farzaneh, and H. Z. Wang. Instrumentation for rapid MR image synthesis. *Magnetic Resonance in Medicine*, 3:33-43, 1986.
4. S. A. Bobman, S. J. Riederer, J. N. Lee, T. Tasciyan, F. Farzaneh, and H. Z. Wang. Pulse sequence extrapolation with MR image synthesis. *Radiology*, 159:253-258, 1986.
5. J. R. MacFall, S. J. Riederer, and H. Z. Wang. An analysis of noise propagation in computed T₂, pseudodensity, and synthetic spin-echo images. *Medical Physics*, 13(3):285-292, May/June 1986.
6. G. L. Bilbro, W. E. Snyder, S. J. Garnier, and J. W. Gault. Mean Field Annealing: A formalism for constructing GNC-like algorithms. *IEEE Transactions on Neural Networks*, 3(1):131-138, January 1992.
7. Garnier, Bilbro, Gault, Snyder, "Magnetic Resonance Image Restoration", *Journal of Mathematical Imaging and Vision*, accepted-forthcoming.